A Physics Extended Essay

INVESTIGATING THE EFFECTS OF WINGTIP FEATHERS ON INDUCED DRAG REDUCTION AND WING EFFICIENCY

Author: Nicolas Deshler

Sponsor: Mr. Tony Godwin

Total Word Count: 3878

Washington International School

Table of Contents

Abstract

Insights derived from biologically-inspired research projects on aerodynamics and fluid dynamics can be beneficial across a broad range of science and engineering fields. The design features of soaring birds' primary feathers are known to benefit the birds' flight efficiency, reducing the energy expenditure required to stay aloft. Previous studies have shown that natural bird feathers attached to the ends of mechanical wings increase wing efficiency more than rectangular wingtip extensions of similar size made of balsa wood.(1) This study examines the effects of feather shape alone on wing efficiency by comparing feather-shaped wingtip extensions (balsawood replicas) to rectangular wingtip extensions composed of the same material. To gather data on the efficiency of different wing configurations the project required building a wind tunnel apparatus capable of accurately measuring lift and drag forces on a wing to determine lift to drag ratios (L/D ratio). These ratios are a quantitative measure of flight efficiency. Computer modeling was used to derive theoretical values for lift and drag forces acting on the mechanical base wing and to validate the experimental instrumentation developed for this project. Lift and drag were measured under various wingtip configurations in the wind tunnel. The selected configurations ensured that differences in efficiency resulted solely from changes in wingtip shape. Each configuration was also tested 0° and 15° angle of attack (AoA) while under constant airflow velocity. My findings show that the shape of wingtip extensions has a significant effect on wing efficiency. Interestingly, at 0° AoA, rectangular balsawood wingtip extensions are consistently more efficient than the balsawood replica feathers, whereas for 15° AoA the balsawood replica wingtip feathers frequently exhibited greater efficiency.

Introduction

Bio-Inspiration Overview

For millennia, the process of evolution has slowly optimized flying organism. Soaring birds, such as hawks, eagles, and vultures, represent the success of nature's handiwork thus far. As highly efficient predatory flyers that seldom flap their wings to stay aloft, they assert their dominion over the skies gracefully gliding overhead. These birds have adapted to use the environment to their advantage, riding thermals and updrafts to increase their altitude without wasting energy. The proficiency of these flyers begs the question; what makes them so successful? Previous studies indicate that much of their flight efficiency can be attributed to a unique feature of their physical wing design. (1) Most soaring birds exhibit long primary feathers extending from the tip of their outstretched wings, creating wingtip slots. These primary feathers are thought to be largely responsible for improved lift and reduced drag characteristics. In essence, soaring birds are designed to minimize the inevitable drawbacks of an inherent property of wings; induced drag.

Induced Drag and Wingtip Vortices

All wings moving through a viscous fluid and producing lift will inherently experience induced drag. In fluid dynamics, and more specifically aerodynamics, Total Drag is composed of two parts. 1. Profile Drag is the resistance generated by molecules colliding over the cross-sectional area of the wing. These collisions transfer momentum between the air molecules and the wing, while also creating friction through fluid layer shearing. 2. Induced Drag is the result of lift created by a difference in pressure between the wing's bottom and top side. As these pressures attempt to equilibrate air slips around the tip of the wing rather than flowing smoothly over the surface. As a result, kinetic energy in this movement of air is lost, yielding induced drag. This movement of air is known as vortex shedding as wingtips typically exhibit corkscrew air patterns of circulating high and low pressure streams, vortices, extending off of

them. Reducing this loss in kinetic energy by correctly harnessing these vortices would result in reduced drag and increased lift.

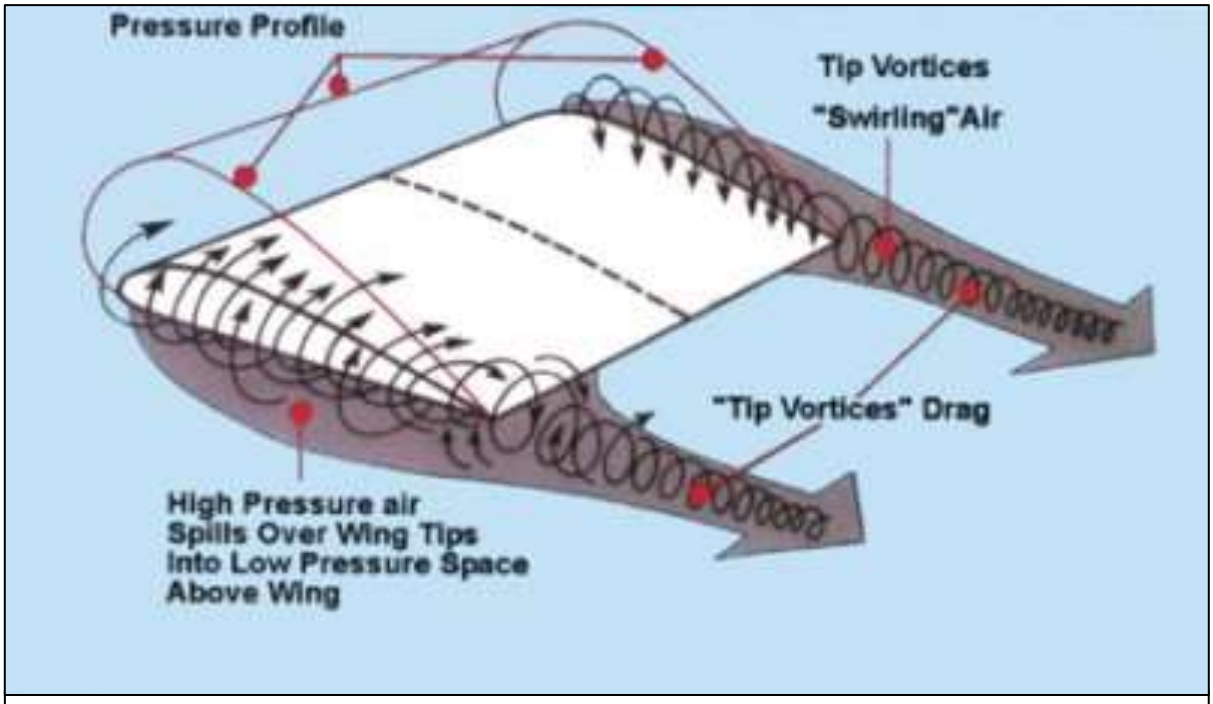

Figure 1.(2) Vortices (induced drag) forming off of wingtips as differences in pressure between the bottom of the wing (high pressure) and the top of the wing (low pressure) equilibrate. The circular motion of the equilibration coupled with the movement of air directly over the wing creates a corkscrew effect generating updrafts and downdrafts in the wake of the wing. In this diagram the pressure profile is also shown to demonstrate where on the wing the pressure difference is greatest.

The Importance of Induced Drag

Other examples in nature demonstrate the significance of the energy available in wingtip vortices. Geese depend on the kinetic energy found in the wingtip vortices to cover long distances during migration. The migratory V-formation allows geese to 'ride' the updraft of the vortices shed by the wingtips of the bird in front, making their demanding flight more manageable.(3) Dragonflies' twin set of wings also exploit the energy present in wingtip vortices. As the leading pair produces it, the aft pair maximizes the use of kinetic energy within the vortex. Dragonflies therefore have among the best maneuverability and flight efficiency of all

insects.[4] Inspiration from these biological adaptations has benefitted mechanized flight. Commercial airliners have been redesigned with curved wingtips called “winglets” to inhibit induced drag and vortex formation. Flight efficiency has improved significantly (nearly 20%) and fuel consumption has dropped as a result.[5] Nature has had millennia to perfect wing shape and tackle the drawbacks associated with induced drag. Understanding the physical process behind the success of soaring birds may reveal more ways in which mechanized flight could improve.

Project Aims and Hypothesis:

The investigation aims to achieve two goals: To verify the validity of experimental precedents that claim wingtip feathers improve the efficiency of a wing, and to determine whether wingtip feather shape has a significant impact on wing efficiency. Experimental precedents, served as a reference point from which this bio-inspired project could advance the overall understanding of the function of wingtip feathers in the scientific community. An experiment conducted by Vance A. Tucker demonstrates that wingtip feathers improve the efficiency of wings by increasing their ratio of Lift force to Drag force. [1] The study also demonstrates that natural primary feathers have a greater effect on induced drag reduction than rectangular balsa wood extensions of similar size. However, the study does not clarify whether the roughly 40% increase in wing efficiency observed at 15 degrees AoA is attributed to the shape of the natural feathers or their distinct material properties. By using machined balsa wood for both the rectangular feather extension and the replica feather extension (replicated 2D profile of a natural primary feather), this Extended Essay focuses exclusively on the effect of feather shape by keeping materials constant.

Building on Tucker’s experiment and principles of wing tip vortex formation process, a hypothesis has been generated: The shape of wingtip extensions is responsible for the improved wing efficiency of natural wingtip feathers over rectangular extensions at high angles of attack. It should be noted that natural primary feathers on soaring birds may not actually maintain constant shape during flight due to their malleability and material structure. In this sense the Extended Essay deviates slightly from realistic conditions.

Theoretical Considerations

Theoretical and Computational Characteristics of the Base Wing

Entering this investigation, preliminary theoretical calculations were necessary to establish how prevalent induced drag is relative to the total drag and to validate experimental values. The ratio of induced drag to total drag of the base wing would help identify whether effects on the induced drag were actually measurable. Had the induced drag been too small on the base wing relative to the total drag, the effect of the wingtip feathers on improving flight efficiency would have similarly been too small to detect. Comparing the values between the base wing's theoretical and experimental lift to drag ratio (L/D ratio) was necessary to validate the experimental method and the collected data further along in the investigation.

Values for the theoretical portion of this investigation were gathered through a combination of software analysis and mathematical calculations. The computer program XFLR5 V6 was used to gather theoretical values for the drag and lift coefficients. The ratio between these values represents the efficiency of the wing. Computational modeling, provides both coefficient values and airflow streamline analyses to predict flight characteristics. Key aerodynamics concepts underlie the formulas and modeling process necessary to determine this ratio: Aspect Ratio, Glide State, and Angle of Attack. They are defined and illustrated below.

Aspect Ratio

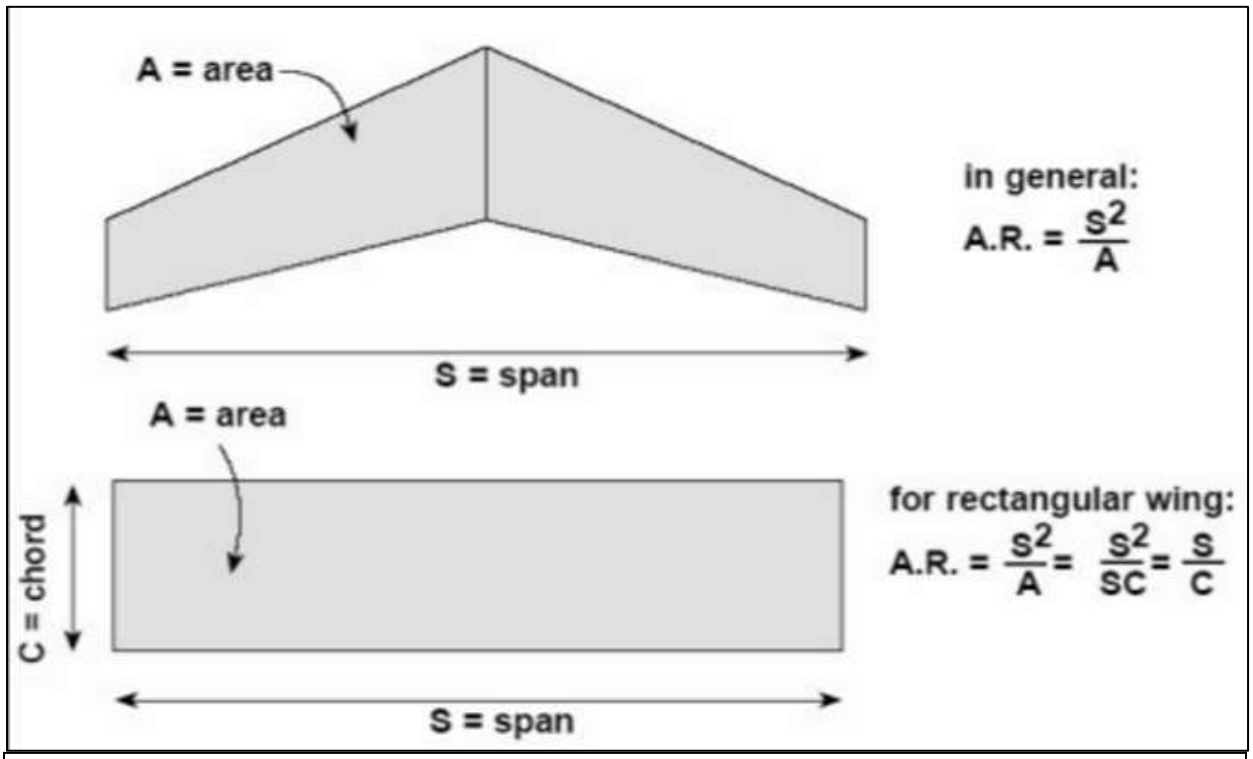

Figure 2. The diagram defines essential wing dimension vocabulary and their relationship with the Aspect Ratio of the wing. For rectangular wings (the shape of the base wing used in this investigation), span is the length of the wing, while chord is the height of the wing when seen from above. Aspect ratio is an important factor associated with induced drag. Generally wings with greater aspect ratios have less induced drag. For this reason, theoretical wings with infinitely long spans have no induced drag. $AR = Span/Chord$

Vector Balance of Forces for a Glider

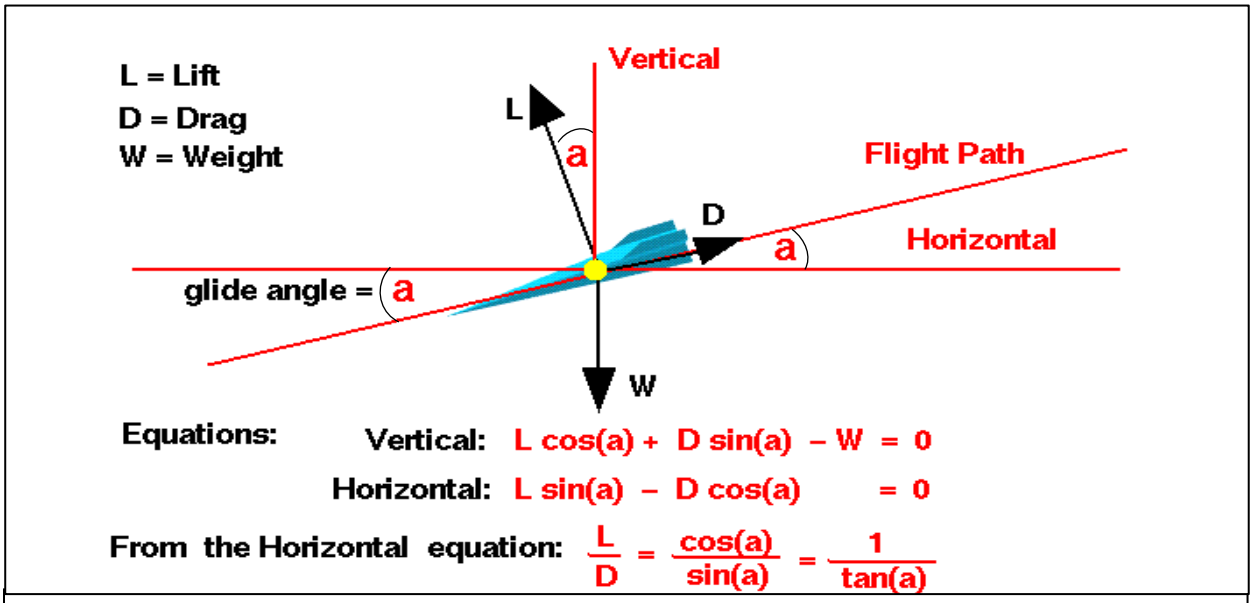

Figure 3. [9] The diagram portrays vector balance of forces for a glider. It is important to note that this situation does not contain a thrust force vector. Glide slope describes the minimum angle the aircraft or bird can fly relative to the horizon without thrust. As soaring birds typically use thermals and updrafts to increase altitude rather than flapping, they are almost permanently in a glide as they fly.

Angle of Attack (AoA) Visualization

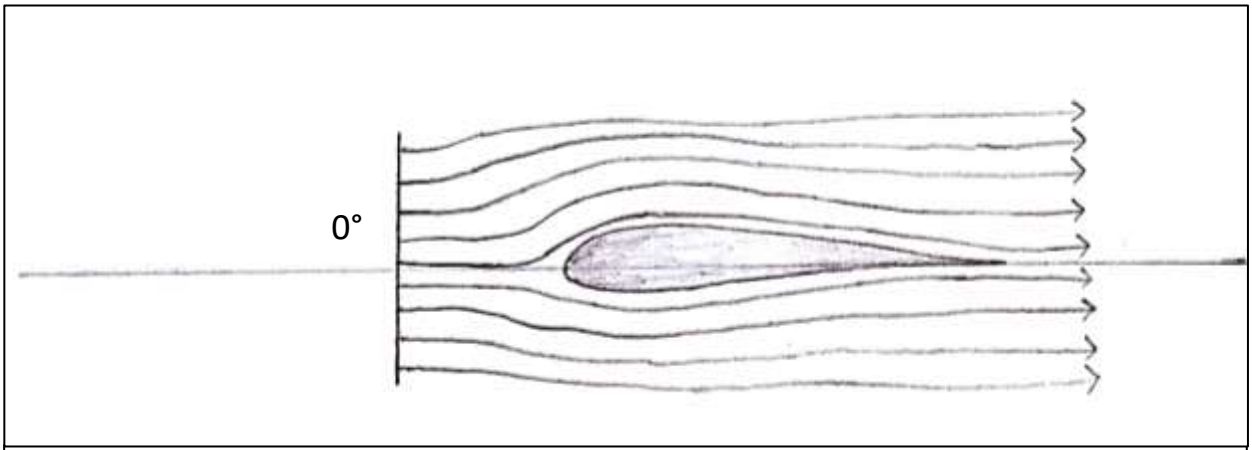

Figure 4. The diagram illustrates airflow around a wing cross-section at 0 Degrees AoA. Here the flow remains considerably laminar as little turbulence is generated by the streamlined airfoil. As a result, minimal drag is produced. In this case, the chord of the wing is parallel to the direction of airflow. Additionally, the boundary layer (not shown) remains in contact with nearly the entire surface of the wing.

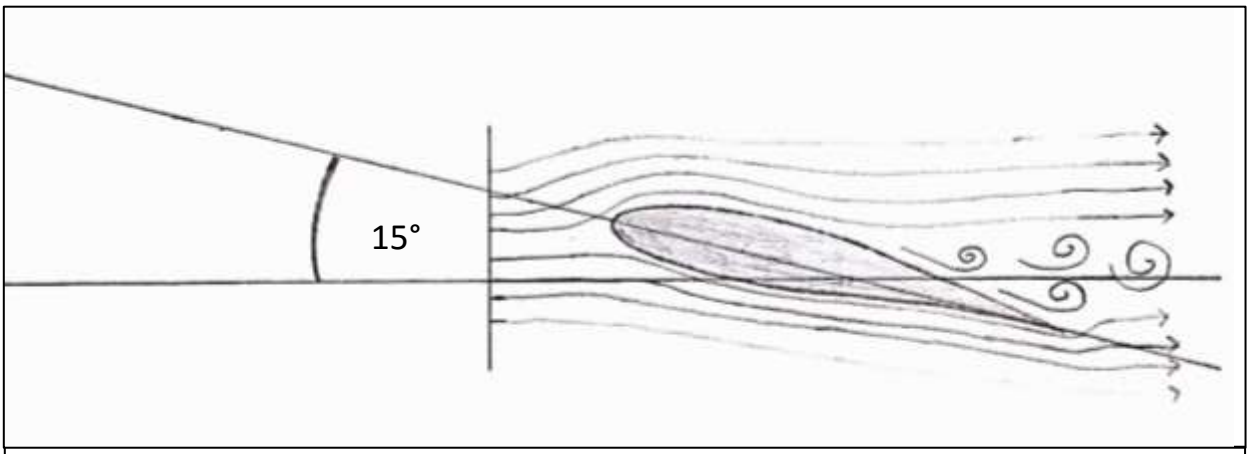

Figure 5. The diagram illustrates airflow around a wing cross-section at 15 Degrees AoA. Although the airflow begins as laminar, it becomes turbulent towards the rear portion of the wing. Here the boundary layer strips away from the top surface of the wing creating vortices. As the cross-sectional wing area in relation to the airflow direction increases, profile drag increases creating greater total drag.

Mathematical Relationships Underlying Aerodynamic Principles

The equation for Lift Force (F_L) on a wing is expressed as,

$$F_L = L = C_L \times \frac{\rho \times V^2}{2} \times A$$

Where, C_L is the coefficient of lift, ρ is the density of the fluid, V is the velocity of the fluid relative to the wing and A is the wing area. (6)

The equation for Drag Force (F_D) on a wing is expressed as,

$$F_D = D = C_D \times \frac{\rho \times V^2}{2} \times A$$

Where C_D is the coefficient of drag, ρ is the density of the fluid, V is the velocity of the fluid relative to the wing and A is the wing area. (7)

As Drag Force is composed of two parts, as expressed earlier, coefficient of drag is also composed of two parts. The equation for Coefficient of Drag (C_D) is expressed as,

$$C_D = C_{Di} + C_{Do}$$

Where C_{Di} is the Coefficient of Induced Drag and C_{Do} is the Drag Coefficient at zero Lift. [8] Zero Lift force on a wing occurs if the wing is at a slightly negative AoA.

C_{Do} corresponds to the profile drag of the wing while C_{Di} is determined through the lift coefficient as induced drag is a result of lift. C_{Di} is expressed as,

$$C_{Di} = \frac{{C_L}^2}{(\pi \times AR \times e)}$$

Where C_L is the Coefficient of Lift, AR is the Aspect Ratio of the wing and e is the efficiency constant which is normally 0.7 for rectangular wings and 1.0 for elliptical lift distribution. [8]

Theoretical Computation, Calculation and Reasoning

Despite its utility, the coefficient of lift has no exclusive formula that expresses its value in different flight situations. Traditionally, physicists determined its value for different wing designs experimentally. However, this method was very time consuming. Thus, modeling software and flow simulation programs have been developed to analyze and approximate coefficient of lift values for different wing designs based on the expected pressure and forces acting on the surfaces of the wing. Therefore, the program XFLR5 V6 was used to calculate the theoretical C_L values of the base wing. To ensure consistency between theoretical calculations and experimental data, aerodynamic constants were established.

Aerodynamic Constants used for Theory and Experiments

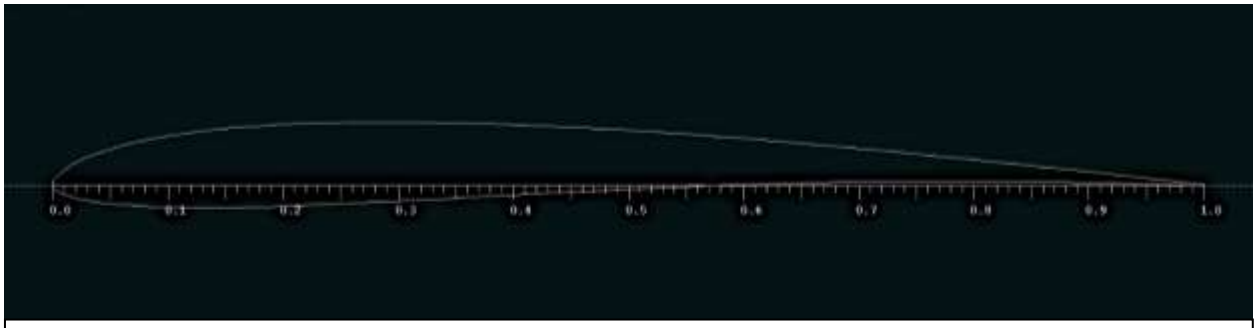

Figure 6. The AG17 Airfoil featured in the diagram above is frequently used for competition style gliders which mimic the un-propelled flight characteristics of soaring birds and are similar in size. Both the AG17 airfoil and soaring bird airfoils are slim to improve penetration in the air and under-cambered to produced exceptional lift.

- Wing Airfoil: AG17
- Constant Airspeed: 3.71 m/s (8.3 mph)
- Base Wing Dimensions:

  > 0.15m Span

  > 0.17m Chord

- Reynolds Number: 51,132

  > Equation $Re = \frac{\rho V l}{\mu}$

  > $\rho\ density\ of\ air$ = 1.225 kgm^{-1}

  > $V\ velocity\ of\ air$ = 3.71ms^{-1}

  > $l\ length\ of\ airfoil\ chord$ = 0.17m

  > $\mu\ dynamic\ viscosity\ of\ air$ = 1.511×10^{-5} Pa s

- E value for Rectangular Wing (Efficiency Factor): 0.70

Calculating C_{Di} of Base Wing

Using XFLR5 V6 it was possible to calculate the Coefficient of Lift values at 0 degrees and 15 degrees Angle of Attack (AoA). The program yielded 0.064 at 0 degrees and 0.379 at 15 degrees. With these Lift Coefficient values it was possible to find the Coefficient of Induced Drag.

Substituting Graphical C_L Values into the C_{Di} equation

0 Degrees AoA

$$C_{Di} = ({C_L}^2)/(\pi \times AR \times e)$$

$$C_{Di} = (0.064^2)/(\pi \times \left(\frac{0.15}{0.17}\right) \times 0.70)$$

$$C_{Di} = 0.0021$$

15 Degrees AoA

$$C_{Di} = ({C_L}^2)/(\pi \times AR \times e)$$

$$C_{Di} = (0.379^2)/(\pi \times \left(\frac{0.15}{0.17}\right) \times 0.70)$$

$$C_{Di} = 0.0740$$

Calculating C_{Do} of Base Wing

As C_{Do} is the drag coefficient at zero lift in the wing, it was possible to use the modelling software to find the AoA where C_L is zero. If C_L is zero when substituted into the Lift equation, then lift will be zero. Furthermore, if lift is zero then induced drag cannot be generated, causing it to be zero as well. So,

$$C_D = C_{Di} + C_{Do}$$

$$C_D = 0 + C_{Do}$$

$$C_D = C_{Do}$$

At -1.75 degrees AoA, the C_L value was zero. Within this analysis C_D was 0.015. As there was no lift, $C_D = C_{Do}$. Therefore, C_{Do} is 0.015 and remains a constant value for AoAs near -1.75 degrees.

Calculating C_D of Base Wing

Having obtained the values for both coefficients, it was possible to find the total drag coefficient for 0 degrees and 15 degrees AoA.

0 degrees AoA

$$C_D = C_{Di} + C_{Do}$$

$$C_D = 0.0021 + 0.015$$

$$C_D = 0.0171$$

15 degrees AoA

$$C_D = C_{Di} + C_{Do}$$

$$C_D = 0.0740 + 0.015$$

$$C_D = 0.0890$$

Induced Drag Calculations

0 Degrees

$\frac{C_{Di}}{C_D} \times 100 =$ Percentage of Induced Drag in Total Drag

$$\frac{0.0021}{0.0171} \times 100 = 12.3\%$$

15 Degrees

$\frac{C_{Di}}{C_D} \times 100 =$ Percentage of Induced Drag in Total Drag

$$\frac{0.0740}{0.0890} \times 100 = 83.1\%$$

Reasoning the Implications of Induced Drag

Total drag is the sum of induced drag and profile drag of a wing. For the modeling above, profile drag is defined as the drag produced by the wing at zero lift. Therefore, profile drag was considered as a constant because there was no way to determine profile drag at AoAs that produce high amounts of lift using the theoretical methods presented above. In reality, profile drag varies with AoA, revealing a limitation of the theoretical calculations. Therefore these calculations were only relevant for AoAs near -1.75 degrees, where lift forces were predicted to be zero. Thus, the percentage of induced drag predicted at 15 degrees AoA was likely inaccurate. In contrast, the percentage of induced drag predicted at 0 degrees AoA (12.3% of total drag) was expected to be close to the actual value. This is because the cross-sectional profile of the wing at 0 degrees AoA is similar (slightly less area) to the cross-sectional profile at -1.75 degrees where zero lift is occurs. Ultimately, the predicted level of induced drag at 0 degrees AoA was likely an underestimate. The theoretical finding that at least 12.3 percent of the total drag was induced drag suggested that the effects of wingtip extensions on minimizing this component of drag were worthy of investigation.

Calculating Expected L/D ratio of Base Wing

Using the values for Coefficient of Lift and Coefficient of Drag it was possible to determine the projected L/D ratio of the base wing. As the equations for lift force and drag force are identical apart from the Coefficients, the ratio of the lift coefficient to the drag coefficient is the same as the ratio of lift force to drag force: $\frac{L}{D} = \frac{C_L}{C_D}$.

<u>0 Degrees AoA</u>

L/D Ratio → $\frac{0.064}{0.0171} = 3.74$

<u>15 Degrees AoA</u>

L/D Ratio → $\frac{0.379}{0.0890} = 4.26$

Streamline Visualization

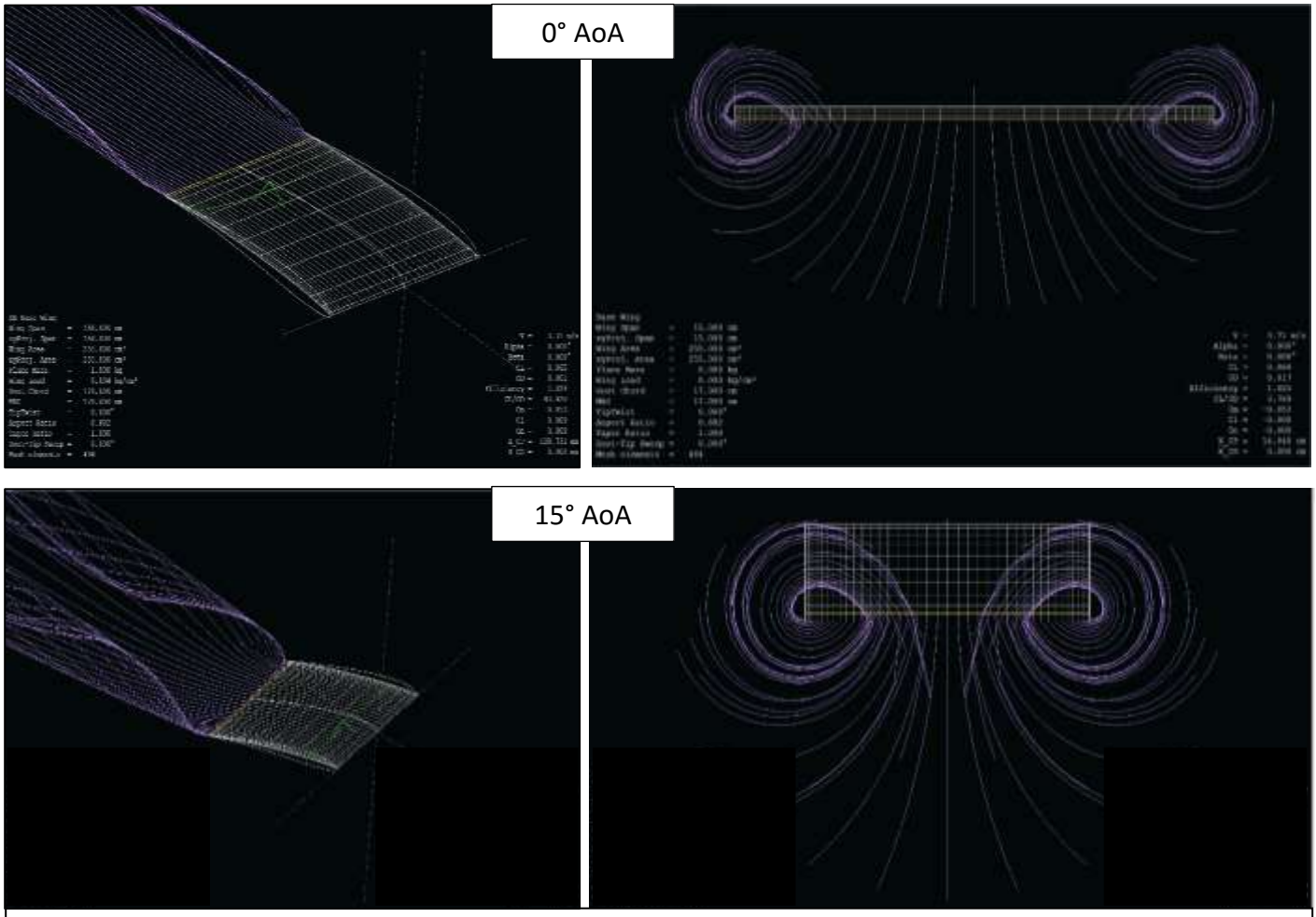

Figure 7. The Figures above show theoretical streamline analyses of the base wing at 0 degrees AoA and 15 degrees AoA (produced in XFLR5 V6). The induced drag of the wing is visually represented by the vortices generated from ends of the wing. In these figures, the geometry of the vortices is telling of the amount of induced drag acting on the wing. The vorticity present at 15 Degrees AoA is drastically more intense than at 0 Degrees AoA. It is evident that the vortices at 15 Degrees AoA are larger in diameter and a exhibit a tighter corkscrew forming closer to the trailing edge of the wing than in the vortices formed at 0 degrees AoA. This suggests an increase in turbulent flow (greater loss of kinetic energy) and thus an increase in induced drag. It is important to recognize that increasing AoA from zero consequently increases both the profile drag and the induced drag of the wing.

Experimental Design

Experimental Apparatus: Function and Development

In fluid dynamics, empirical data often deviates considerably from theoretical values. This is because the equations used to model complex fluid interactions and behaviors in different situations are oversimplified. Therefore, it is important to verify or challenge the theory through empirical experimentation in order to obtain a thorough and realistic understanding of the physical factors at play. The experimental apparatus developed for this investigation was composed of a multi-configurable wing and a wind tunnel.

The Multi-Configurable Wing

The base wing was made of dense insulation foam, cut to the shape of an AG17 airfoil using a hotwire cutter. It was then covered tightly in transparent packing tape to avoid unusual fluid-solid surface interactions on the porous foam. The span and chord of the wing were 0.15m and 0.17m respectively. The base wing was also equipped with five equally-spaced attachment points along the end of the wing. These attachment points were designated for the wingtip feathers. Five identical rectangular wingtip feather extensions were laser cut out of 2mm balsa wood at the Johns Hopkins University senior design lab. They were then beveled evenly on the edges with sandpaper to streamline their profiles. Similarly, 5 identical feather-shaped wingtip extensions were cut out of balsa wood. They were of the same length as the rectangular extensions and were beveled. The feather-shaped wingtip extensions were cut to the same shape as the outline of an actual bird feather. In this investigation, the fifth primary feather of the California Condor was selected for replication, due to the bird's superior soaring-flight abilities (see **Figure 8**). The multi-configurable wing allowed for adjustable spacing between extensions. Relative to the base wing, the balsawood wingtip extensions were considerably larger. The multi-configurable wing was purposefully disproportionate to an actual condor

wing. By making the wingtip extensions larger in length than the base wing, their effect would be more noticeable when gathering data. It is also important to note that the multi-configurable wing did not have the variability of a real bird wing as birds typically fan out their feathers horizontally and vertically. This unique movement was not made an option in the apparatus, and hence, was not tested.

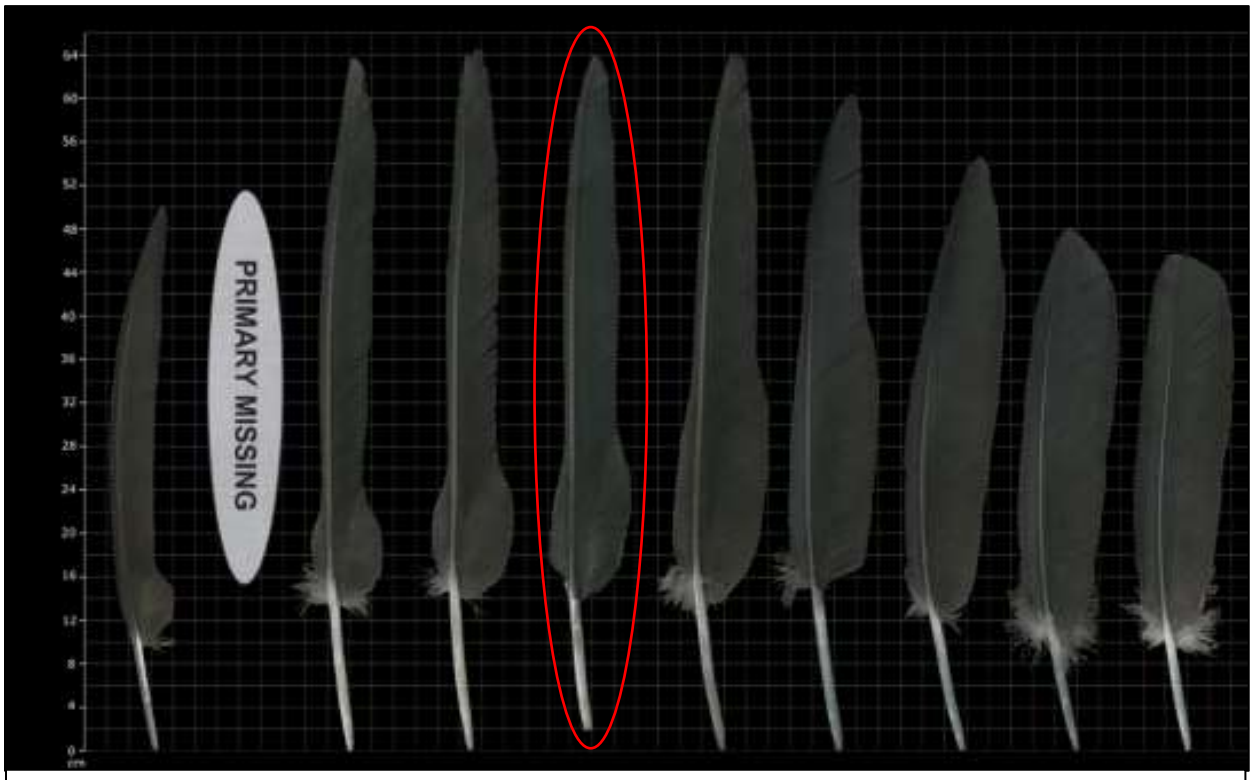

Figure 8. [10] (Diagram not to scale) The diagram exhibits the primary feathers of an adult California Condor ordered from the front of the wing to the back (looking left to right). Feather-shaped balsawood extensions were modeled after the fifth primary feather circled in red.

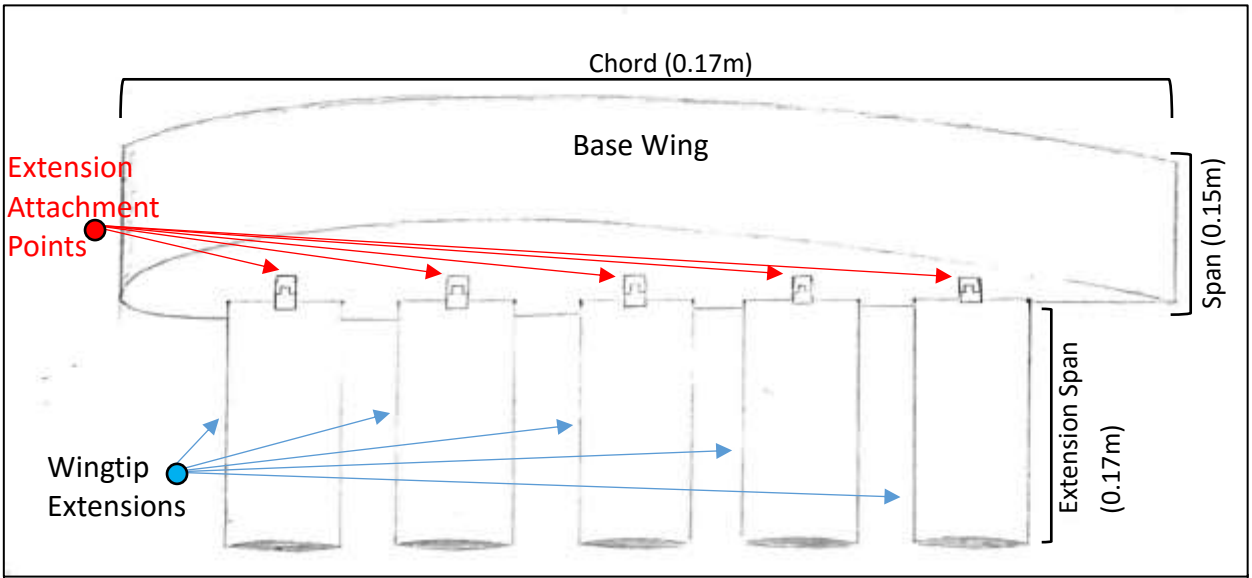

Figure 9. (Diagram not to scale) The schematic shows the components and dimensions of the multi-configurable wing. The extension attachment points were created out of LEGO connectors. These were sanded to a streamlined profile to reduce drag and fitted into the foam and extensions. This way each extension was easy to swap for different configurations during the tests. The chord of the rectangular extensions is 0.025m (not shown above). The chord of the feather-shaped extensions (not shown above) was inconsistent over the span of the extension (0.17m) because of its irregular geometric profile. However the maximum chord was also 0.025m allowing for approximately 1 cm of spacing between each extension.

The Wind Tunnel

The wind tunnel was designed to provide controlled and consistent airflow over the wing while also providing a means of conducting lift and drag force measurements on the wing. Certain design features of the wind tunnel helped improve the quality of airflow. Firstly, the fan generates lower pressure at the back of the wind tunnel to draw a uniform volume of air in through the front at the same speed in all sections of the rectangular prism. Secondly, laminar flow (flow with minimal turbulence) was approached by placing a honeycomb-shaped mesh at the tunnel entrance made out of 2.5 cm diameter PVC piping. Thirdly, the wind tunnel was made entirely airtight using caulking and weather stripping with exception of the entry and exit airways. Therefore, steady flow was maintained, as air was not drawn from different spots on the wind tunnel. Acrylic windows were placed on the top and side of the wind tunnel to allow

for qualitative observations of the airflow around the wing. The portion of the wind tunnel dedicated to acquiring quantitative data for the lift and drag forces acting on the wing is somewhat complex.

As noted in the Physics section of The International Baccalaureate Extended Essay Guide: “The domains of aerodynamics and hydrodynamics are theoretically and experimentally very demanding; for example, the construction of wind tunnels can be problematic and time-consuming. A topic within these domains must be chosen and defined very carefully.” The complexities associated with an investigation in aerodynamics, particularly in the experimental process, were fully recognized. In the end, the wind tunnel design required many hours to ensure it was effective, durable and airtight. Cutting the acrylic to size posed problems as scoring the material was often insufficient to produce a clean break. An initial version of the wind tunnel had an excessively large cross-section and an underpowered fan. With this set up the airflow through the tunnel was travelling at $<0.45\ ms^{-1}$ (1 mph). This produced no detectable lift or drag forces on the wing with the available measurement apparatus and did not match the airspeed or Reynolds number of a bird in flight. As a result the effective cross-sectional size of the wind tunnel with internal panels had to be reduced and the former fan replaced with one of greater size, power, and volume output. This modification drastically improved the airspeed, bringing it up to $3.71\ ms^{-1}$ (8.3 mph) ± 0.05. Despite these challenges, the opportunity to gather accurate and precise measurements on the effects of wing-tip extensions made possible by a wind tunnel, overrode the extensive demands for time and technical expertise.

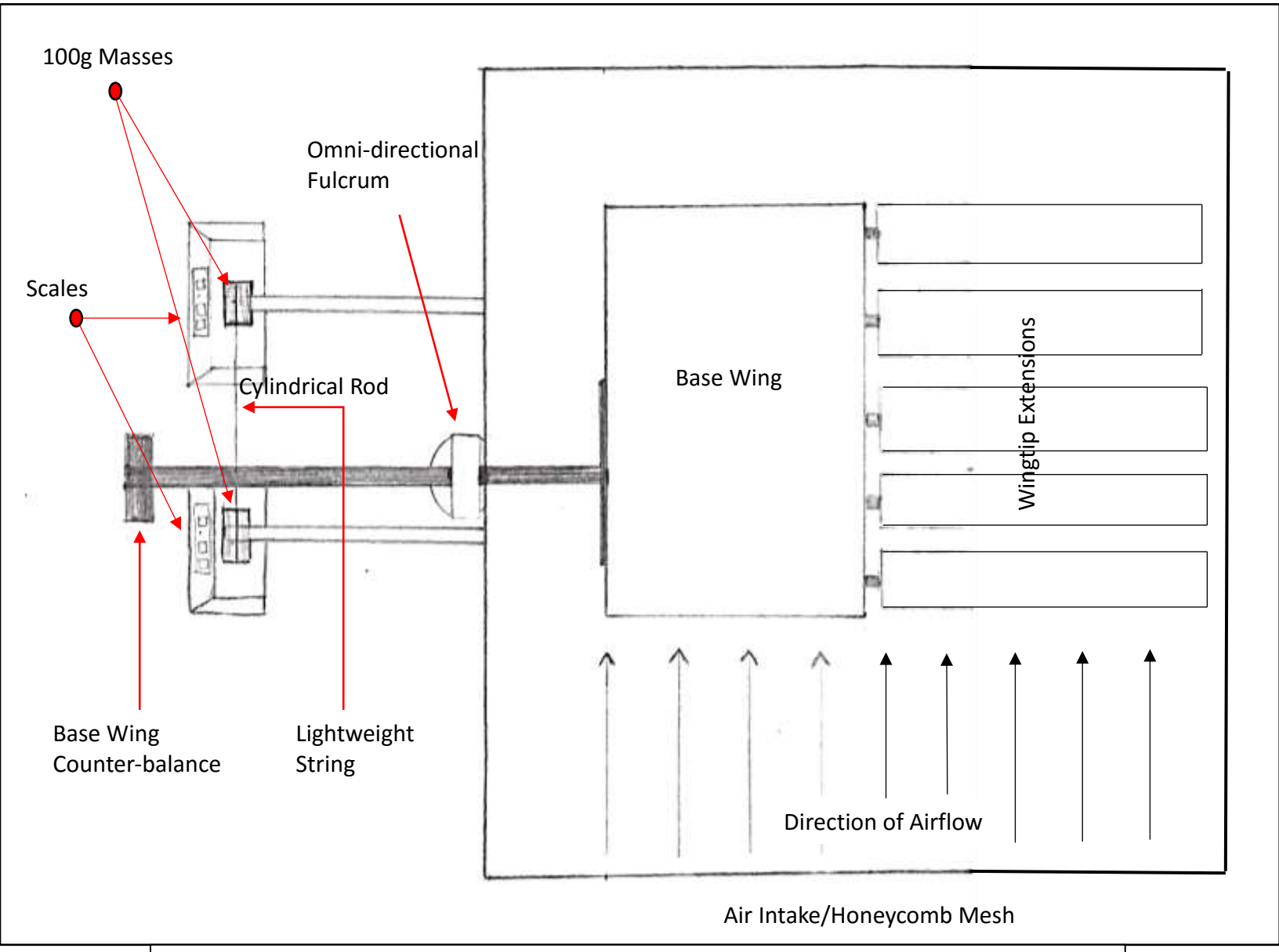

Figure 10. (*Top View* -- Diagram not to scale) Overall the airflow passes through a cross sectional rectangular prism of 60cm in length, 45cm in width, and 14cm in height. A cylindrical rod is inserted through one of the side panels on the wind tunnel so that one end of the rod is within the airflow chamber and the other protrudes out of the side of the tunnel. The base wing slides horizontally onto the end of the rod situated inside the wind tunnel. The protruding end is connected to an Omni-directional fulcrum that allows the rod to pitch up and down as well as side to side (x and y directions). The forces acting on the rod in these directions propagate through strings connected to a pulley system. These strings lift masses that are placed on scales that provide readings for the lift and drag on the wing. The airspeed within the wind tunnel was calculated by placing an anemometer in the center of the wind tunnel while it was empty and averaging the recorded airspeeds. The average was ultimately 3.71 ms-1 (8.3 mph) ± 0.05

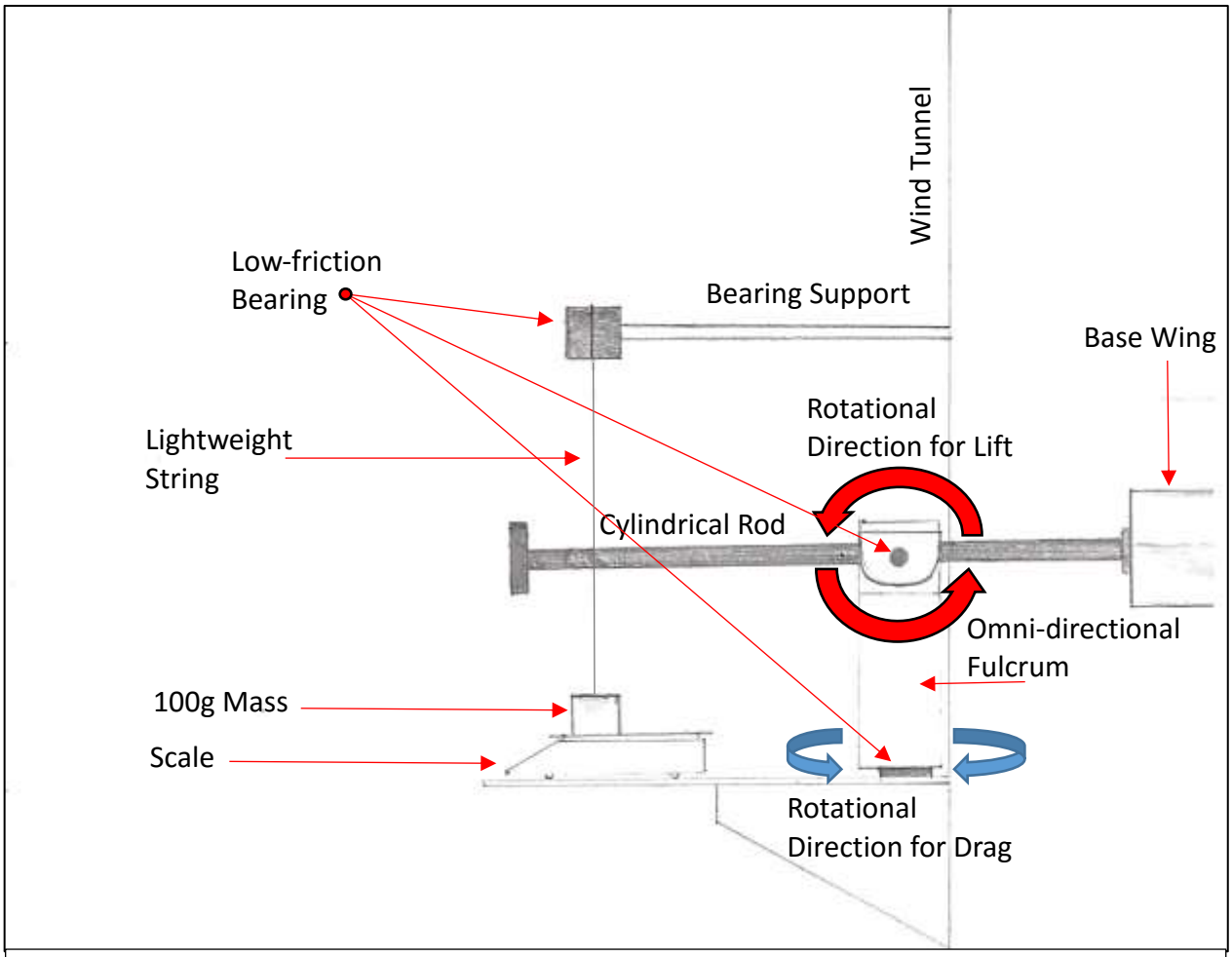

Figure 11. (*Front View* -- Diagram not to scale) The measurement apparatus uses tension forces in lightweight strings to transfer the aerodynamic forces on the wing to measureable weights on the scales. A pulley system using low-friction skateboard bearings directs the forces appropriately such that the weight measurements describe lift and drag forces. The wing is counterbalanced in the wind tunnel by a weight at the protruding end of the rod. The lightweight strings are taught around the rod so that as the airflow passes over the wing, it remains stationary. This is crucial as the lift and drag forces would change if the wing were not directly perpendicular to the flow direction. It is also important to note the potential sources of error in the measurement apparatus. First, the lightweight strings are not perfectly inextensible. Therefore, the tension force is likely diluted slightly which would affect the values registered on the scale. Secondly, although the bearing pulleys basically remain stationary during experimentation, it is possible that slight friction within the bearings would reduce the forces registered by the scale as the string stretches. Finally, as the dowel is made of wood, it is susceptible to flexing under the strenuous forces, which would also skew results. All of these potential sources of error would likely have marginal effects on the collected data.

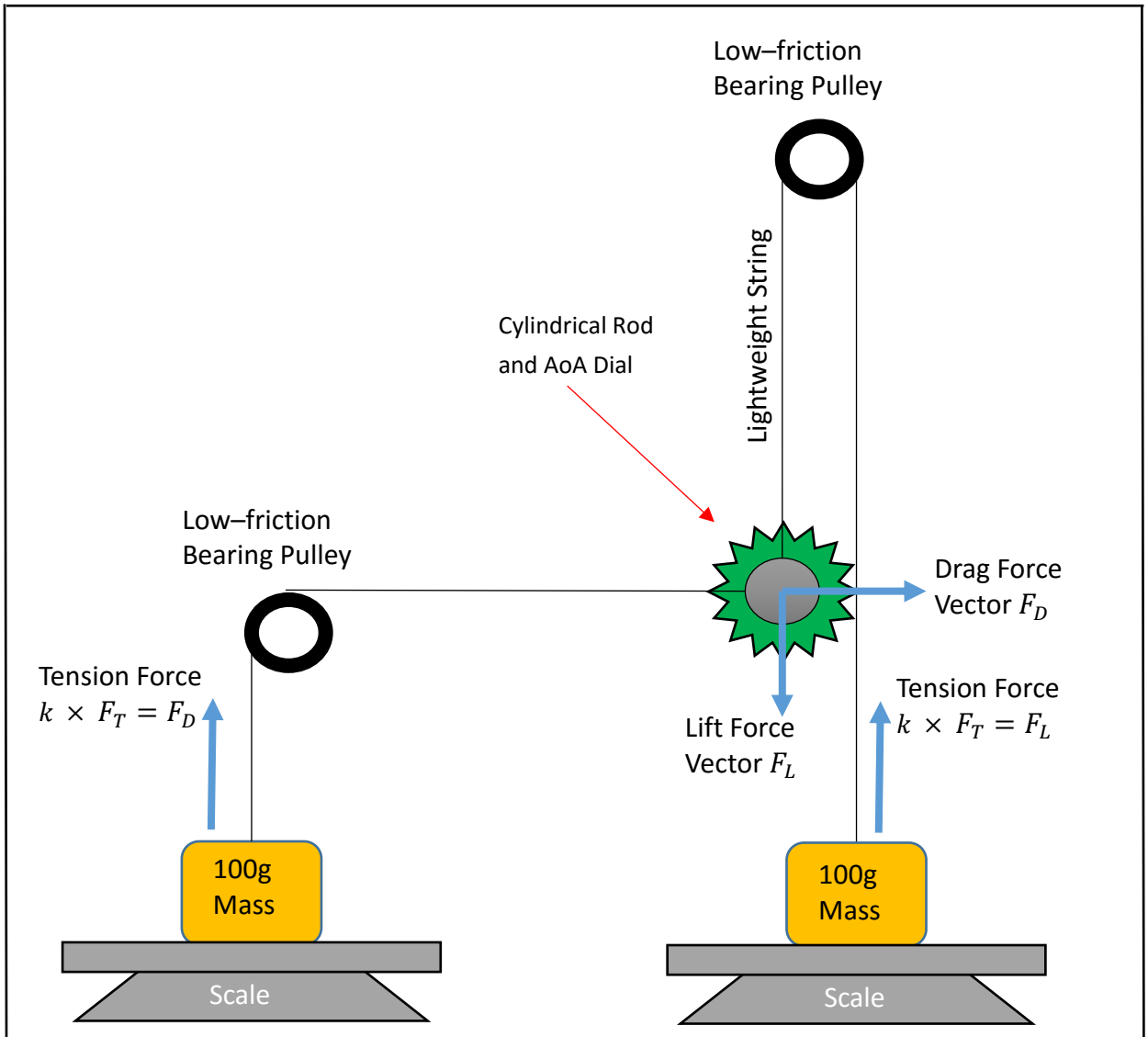

Figure 12. (*Side View* – Diagram not to scale) Two fixed pulleys, one above and one horizontal to the rod, are individually connected to the rod using lightweight string. The other ends of the strings are connected to heavy 100g masses situated on sensitive scales that measure to the nearest hundredth of a gram. The string is taught between the rod and the masses so that when air passes through the wind tunnel, the wing does not shift position thus improving the accuracy of the lift and drag force measurements. As the wing experiences aerodynamic lift and drag, these forces are translated through the string tension causing the scales to register a difference in weight. The aerodynamic forces are therefore proportional to the gravitational force registered on the scales as torque occurring between one end of the fulcrum and the other must be factored in. This proportion is represented by the coefficient k. As scales are used to determine the forces, the units of all lift and drag measurements are described in grams. By rotating the rod with a calibrated dial it was possible to systematically change the AoA of the wing and still conduct lift and drag force measurements.

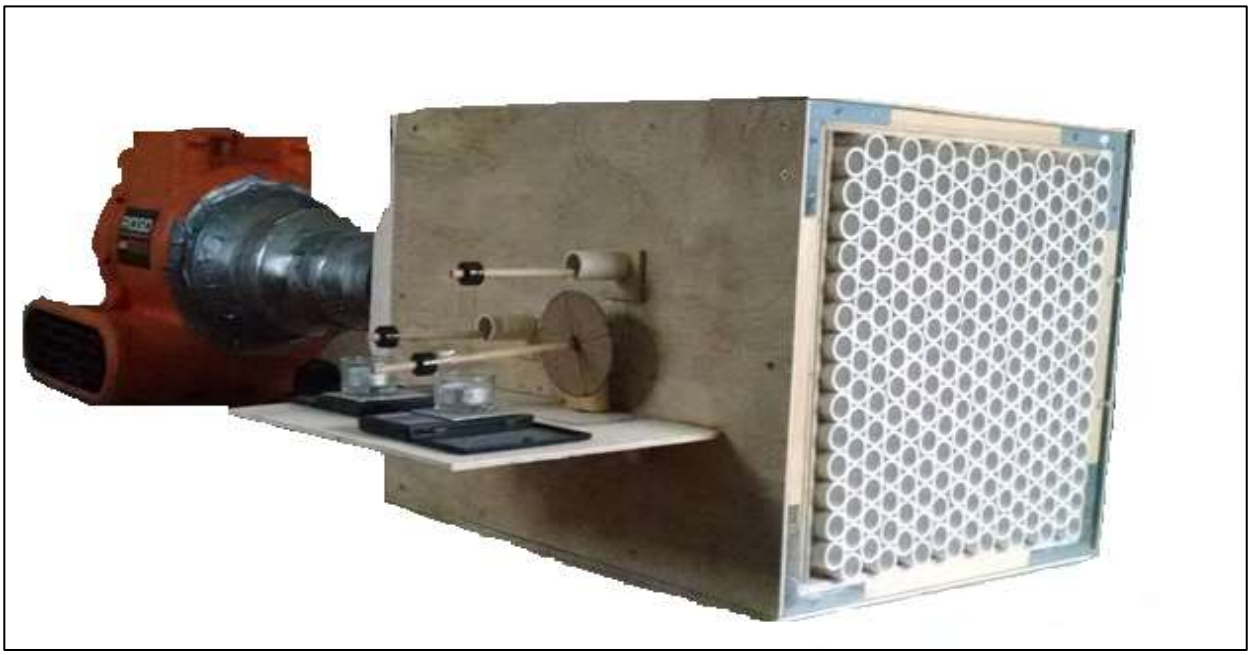

Experimental Procedure

The experimental procedure for this investigation managed 3 independent variables that were crucial for examining the effect of feather shape on the L/D ratio: Extension shape (feather-shaped vs. rectangular), Angle of Attack (AoA), and feather spacing. Two wingtip extension shapes were chosen to determine whether the form of soaring birds' feathers serve to improve their flight efficiency. The rectangular extensions were chosen for their basic geometry. The feather-shaped extensions were replicas of the California condor's primary feather. AoA of 0 and 15 degrees were chosen for separate reasons. 0 degrees AoA is a common baseline flight position as it is typically close to the flight orientation seen in gliding. Fifteen degrees AoA was chosen as another flight parameter as the precedent study by Vance A. Tucker demonstrates the greatest difference between real and rectangular feather extensions occurred at 15 degrees AoA. Increasing the number of feathers (reducing the spacing between them) served to maximize the effect of the different feather types to highlight any differences in their performances.

Discovering the effects of wingtip extension shape on the L/D ratio or efficiency of a wing required a systematic change of the independent variables and their effects on lift and drag forces. For feather-shaped and rectangular extensions, measurements were made with different numbers of feathers at 0 and 15 degrees angle of attack. The number of feathers at which measurements were made were 1, 2, 3, and 5. Measurements on 4 feathers were not performed as their configuration could not evenly space the feathers and thus was not standardized among the other numbers of feathers. As the number of feathers increased, the spacing between them decreased.

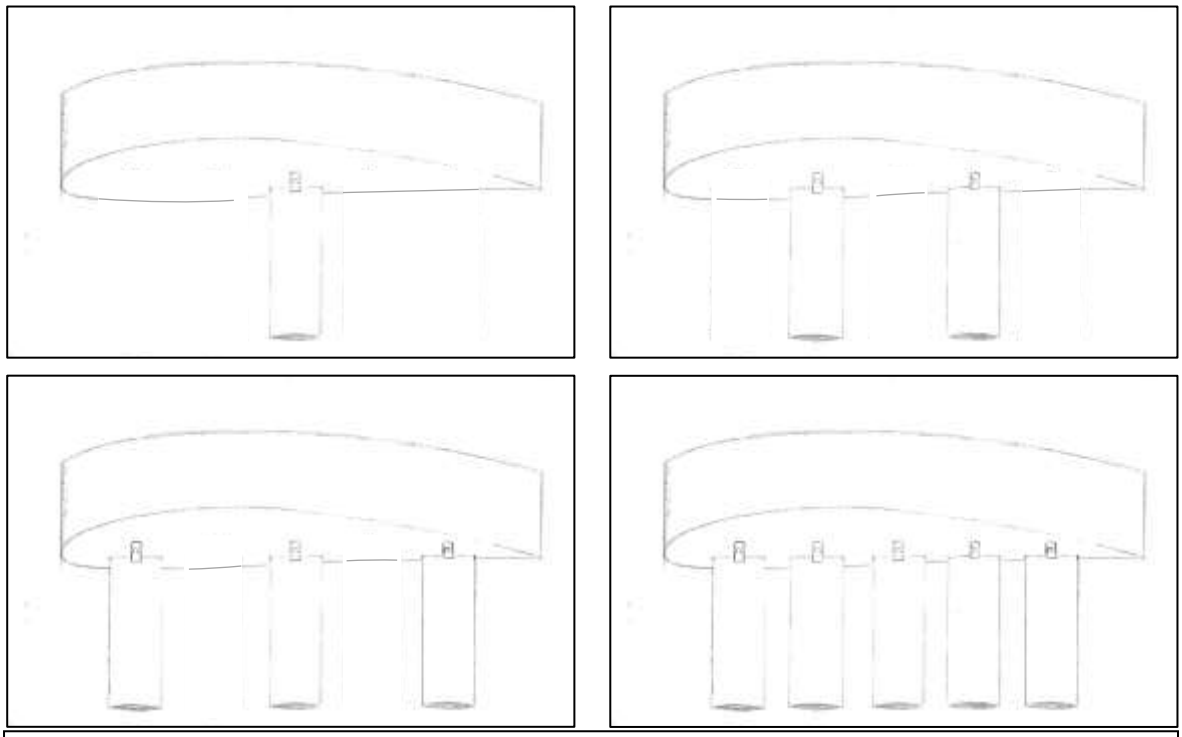

Figure 14.1 (above) and 14.2 (below). (Diagrams not to scale) The diagram above illustrates the four wingtip configurations used in the wind tunnel. In each case the wingtip extensions are placed equidistant from one another and symmetrically. For this reason, a configuration involving four wingtip extensions was excluded from the experiment. Below a photograph of the actual multi-configurable wing is shown with both feather-shaped and rectangular extensions.

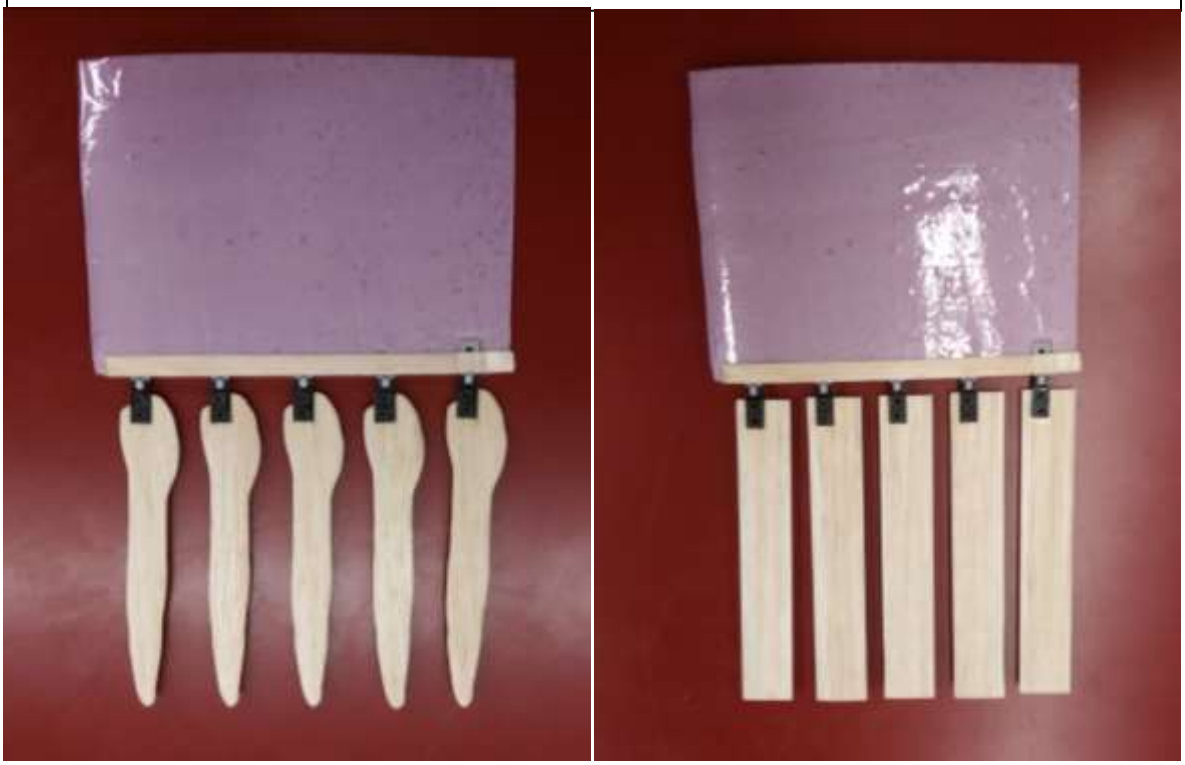

Results

Validation of Experimental System

To determine whether the experimental setup produces reliable results, the L/D ratio of the base wing were gathered experimentally at 0 degree AoA and compared to the theoretical value. Ten independent measurements were taken for each set of conditions and averages calculated. Table 1 shows that the data are quite consistent as the experimentally determined average L/D ratio for the base wing is 3.72 ± 0.04. This value corresponds very closely to the base wing's theoretically predicted L/D ratio of 3.74 determined in the Theoretical Considerations section above. The reproducibility of the measurements and their consistency with theoretically produced L/D ration values demonstrates the dependability and utility of the wind tunnel and force measuring devices used throughout this investigation. It should also be noted that all the data measurements and tables indicating lift and drag forces are in grams. Although this is not the appropriate unit for a force, the objective of this investigation was to determine the ratio of lift to drag forces. Therefore, the coefficient required for the conversion between grams and Newtons is unnecessary.

Table 1: *Base Wing Efficiency at 0° AoA*

Trials	**Lift (g) ± 0.1**	**Drag (g) ± 0.1**	**L/D**
T1	4.8	1.3	3.69
T2	4.6	1.3	3.54
T3	4.6	1.2	3.83
T4	4.8	1.3	3.69
T5	4.4	1.2	3.67
T6	4.6	1.2	3.83
T7	4.6	1.2	3.83
T8	4.5	1.3	3.46
T9	4.6	1.2	3.83
T10	4.6	1.2	3.83
Average	**4.61**	**1.24**	**3.72**
Standard Error of the Mean	0.0359	0.0155	0.0410

Effects of Wingtip Extension Shape on Wing Efficiency

The purpose of this investigation was to test the hypothesis that the shape of wingtip extensions increases wing efficiency. To do this, a range of wingtip configurations were tested to maximize the chances of detecting discernable differences in efficiency between wingtip extension shapes. L/D ratios were derived from Lift (L) and Drag (D) force measurements (See appendix for data) collected with the experimental wind tunnel apparatus designed and constructed for this investigation. Table 2/Graph 1 and Table 3/Graph 2 show L/D ratios for feather-shaped and rectangular wingtip extensions as the number of extensions was increased from 1 to 5, at 0 degrees and 15 degrees AoA, respectively.

The rectangular wingtip extensions were consistently more efficient at low (0 degrees) AoA (Table 2/Graph 1). At each configuration, from one to five wingtip extensions, the difference in L/D ratios between rectangular and feather-shaped extensions ranged from .42 to 1.45, but were always greater with rectangular extensions compared to feather-shaped ones. Interestingly, this is similar to the findings of Tucker who observed that rectangular wingtip extensions had slightly higher efficiencies than natural feathers at low AoAs.

Table 2: *Wing efficiencies (L/D Ratios) at 0° AoA*

Feather Number	Rectangular L/D	Feather-shaped L/D	Δ(L/D)
1	5.02 ± 0.034	3.57 ± 0.030	1.45
2	3.82 ± 0.011	3.34 ± 0.032	0.48
3	4.03 ± 0.031	3.61 ± 0.031	0.42
5	4.01 ± 0.015	3.03 ± 0.033	0.98

Graph 1: *Wing efficiencies (L/D Ratios) at 0° AoA*

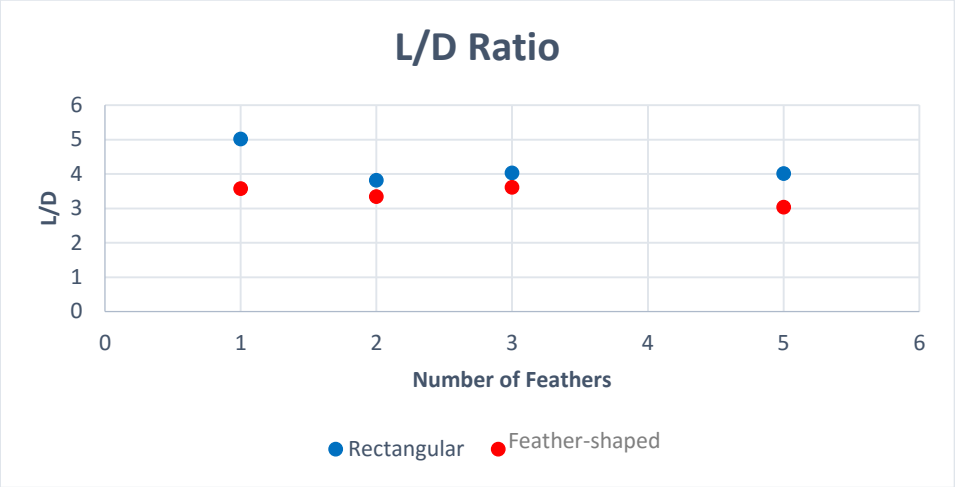

The experiments at 0° AoA provided additional confidence that the experimental set up in this investigation was a reliable system for addressing the hypothesis under study. To test the hypothesis directly, the AoA was changed to 15° and wing efficiencies were compared between wingtip extension shapes to determine whether shape, *per se*, improved wing efficiency at high AoA. Under this configuration, feather-shaped wingtips were consistently more efficient than rectangular extensions. At 15° AoA, the greatest differences in L/D ratio were found at 1 feather (0.34) and 2 feathers (0.36) (Table 3/Graph 2), which led to 14% and 16% increases in efficiency, respectively. At higher feather numbers (3 and 5) feather-shaped tips continued to be more efficient than their rectangular counterparts, although to a lesser extent (Table 3/Fig. 3). Although the improved efficiency percentages at 1 and 2 extensions were somewhat lower than the roughly 40% increase in efficiency observed with natural feathers by Vance A. Tucker's experiment [(1)], they clearly demonstrate that wingtip shape alone plays a significant role in increasing wing efficiency at high AoA. These data show that the feather-shaped shape, in itself, can enhance wing efficiency at high AoA, consistent with the hypothesis. However, the extent of this improvement does not appear to be as high as shown in Tucker's previous study. Therefore, material properties of natural feathers may also contribute to this improvement. The material properties of the surface of an object in flight (including the microscopic-structure and morphology) often affect the boundary layer conditions. Therefore, it is possible that the

composition of bird feathers encourages the boundary layer to remain attached over a greater amount of surface area, effectively decreasing drag.

Table 3: *Wing Efficiencies (L/D Ratios) at 15 0° AoA*

Feather Number	Rectangular L/D	Feather-shaped L/D	Δ(L/D)
1	2.36 ± 0.007	2.69 ± 0.012	0.33
2	2.32 ± 0.012	2.58 ± 0.010	0.36
3	2.55 ± 0.017	2.35 ± 0.012	-0.196
5	2.24 ± 0.021	2.27 ± 0.005	0.029

Graph 2: *Wing Efficiencies (L/D Ratios) at 15 0° AoA*

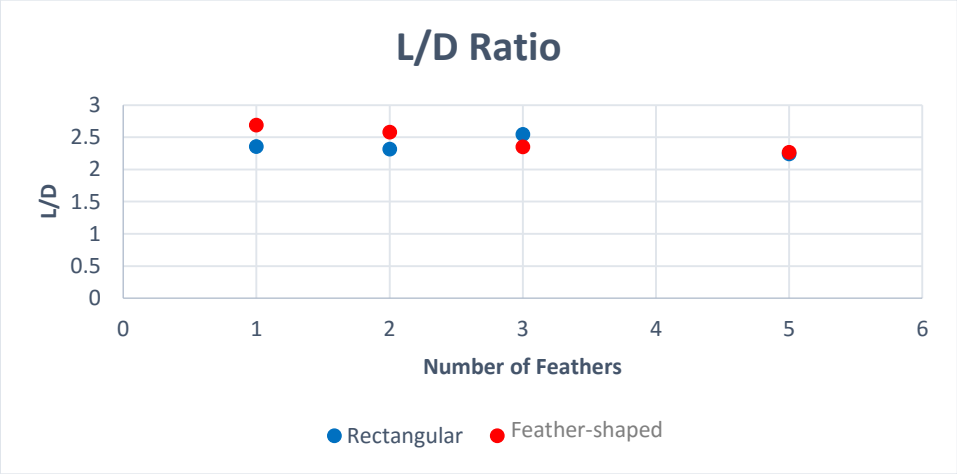

Increases in efficiency can be the result of increases in lift forces, decreases in drag forces or a combination of both as the efficiency is dictated by the L/D ratio. Interestingly, the enhanced L/D ratio of the feather-shaped extensions observed at high AoA with one wingtip extension was a combination of both an increase in lift and a decrease in drag relative to the rectangular extension. However, this occurred to different extents with various configurations revealing no definitive trend in this regard (Refer to appendix tables).

Discussion

In this investigation it was shown that wingtip extension shape has a substantial effect on wing efficiency. At low angles of attack, L/D ratios of rectangular extensions were greater than L/D ratios of feather-shaped extensions. In contrast, at high angles of attack, L/D ratios of feather-shaped extensions were greater than those of rectangular extensions. There are a number of potential explanations behind these findings. Reasoning for these explanations is based on principles and phenomena of fluid dynamics.

The interaction between wingtip extensions and wingtip vortices is an important focus in this discussion. Comparing the L/D ratios shown in Graph 1 and Graph 2 reveals that rectangular extensions consistently increase the base wing efficiency at 0 degrees AoA. While this increase may seem to be due to the longer wingspan and thus greater aspect ratio exploiting the Bernoulli Effect, this is not likely to be the case. The wingtip extensions were created with symmetrical airfoils. At 0 degrees AoA symmetrical airfoils do not produce lift, as the distance from the leading to the trailing edge is identical on the top and bottom of the wing. Therefore, there is no difference in pressure between the top and bottom of the wingtip extensions hence, no lift is produced. Instead, it is speculated that the spacing between the feathers diffuses the vortex generated at the end of the base wing by preventing pressure equilibration and catching the updraft. This diffusion is likely to maximize the lift and simultaneously reduce drag by harnessing the kinetic energy of the vortices, thereby improving the L/D ratio. This process has been shown to be the case in an apparatus similar to the one used in this investigation in which extremely small helium bubbles flowing within the wind tunnel were tracked to analyze vortex diffusion. [(1)]

Even though feather-shaped extensions produced greater L/D ratios than rectangular extensions at 15 degrees AoA, both extension shapes exhibited lower L/D ratios than the base wing at 15 degrees AoA. One potential explanation for this could involve vortex formation upon the wingtip extensions themselves. Symmetrical airfoils do generate lift at AoAs greater than xero. As both wingtip extension shapes were created with symmetrical airfoils, both types will

inherently generate their own lift and consequently induced drag at 15 degrees AoA. It is likely that the feather-shaped extensions produce less induced drag due to the elliptical lift distribution of its shape. Elliptical lift distributions are known to reduce the intensity of wingtip vortex formation and therefore reduce induced drag by minimizing the difference in pressure at the wingtips. This is achieved by tapering the tip of a wing. Interestingly, the feather-shaped extension is tapered, producing more lift at the base of the extension and less at the end.

One qualitative observation made during configuration tests further supports the likely possibility that there was significant interaction between the base wing vortices and the wingtip extensions. Throughout all of the trials where feather-shaped or rectangular wingtip extension were attached to the base wing, there was noticeable flutter among the extensions. This could be the result of the vortices acting upon the extensions or it could be an arbitrary turbulent flow, reflected in the high Reynolds Number at which the tests were conducted. This aspect could be one for further investigation to understand the dynamics of vortices-wingtip interactions.

Conclusion and Future Directions

In this investigation, I have shown that feather-shaped extensions modeled after soaring birds' primary feathers have distinct effects on wing efficiencies, flying at low AoA (cruise flight attitude) and high AoA (climbing flight attitude). Plausible explanations are presented for these distinct differences. While shape alone does not account for the entire efficiency increase observed with natural feathers in a previous study, the bio-inspired shape used in this study has unique qualities that could serve to enhance flight performance of mechanical aerial vehicles.

Future initiatives may be taken to expand on this investigation. For example, qualitative visualization and analysis of the interaction between wingtip extensions and wingtip vortices could be achieved by passing smoke through the wind tunnel apparatus to observe the airflow. Computational Fluid Dynamic analysis of the various types of vortices generated by increasing or decreasing AoA and changing the wingtip configurations would also be an intriguing path to pursue in the future. Using real feathers with this particular experimental set up would help identify other characteristics of natural feathers that help increase wing efficiencies. This would also be useful to verify or challenge the validity of experimental precedents.

Appendix

Figure 1: Multi-configurable Wing with Extensions Positioned in the Wind Tunnel

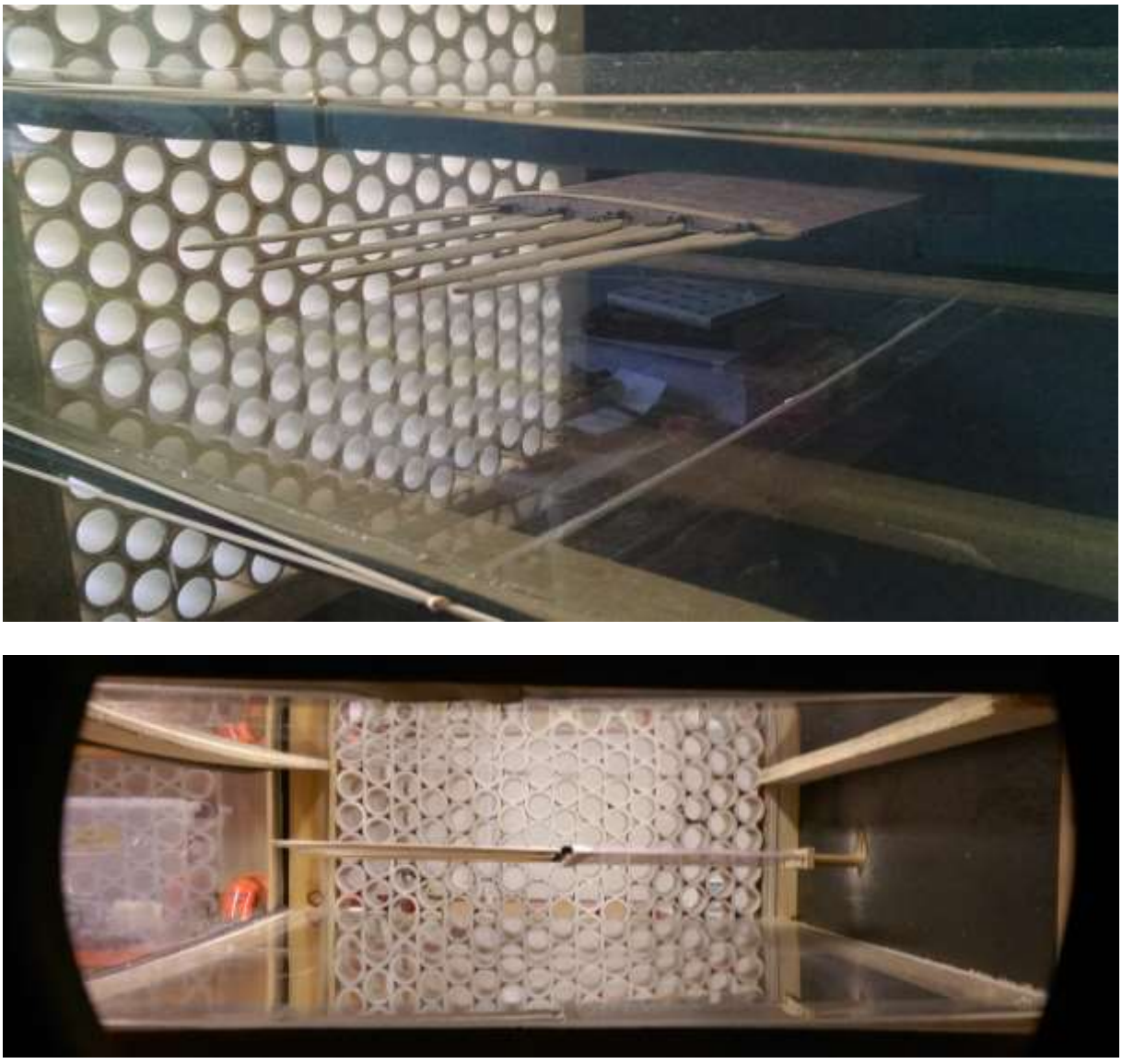

0 Degrees Angle of Attack

Table 1

Lift of Rectangular Extension configurations at 0^o AOA

Trials	Lift with 1 Feathers (g) ± 0.1	Lift with 2 Feathers (g) ± 0.1	Lift with 3 Feathers (g) ± 0.1	Lift with 5 Feathers (g) ± 0.1
T1	10.2	10.2	16.0	17.6
T2	10.0	9.3	15.9	18.0
T3	9.6	9.5	15.7	17.0
T4	10.1	9.8	15.8	17.2
T5	9.8	9.4	16.3	17.2
T6	10.0	9.6	16.2	17.7
T7	9.9	9.2	15.7	17.3
T8	10.2	9.6	15.5	17.4
T9	10.0	9.6	15.9	17.4
T10	10.0	9.6	16.3	17.3
Average	**10.0**	**9.6**	**15.9**	**17.4**
Standard Error of the mean	0.055	0.084	0.081	0.087

Table 2

Lift of Feather-shaped Extension configurations at 0^o AOA

Trials	Lift with 1 Feathers (g) ± 0.1	Lift with 2 Feathers (g) ± 0.1	Lift with 3 Feathers (g) ± 0.1	Lift with 5 Feathers (g) ± 0.1
T1	6.7	9.1	13.8	13.1
T2	6.9	9.1	12.9	13.2
T3	7.0	9.0	13.1	12.9
T4	6.3	8.9	12.8	12.6
T5	6.6	9.0	13.7	12.8
T6	6.5	9.2	13.0	12.0
T7	7.0	8.9	13.0	12.2
T8	6.9	9.0	12.9	12.1
T9	7.0	8.9	13.0	12.5
T10	6.6	8.6	12.9	12.0
Average	**6.8**	**9.0**	**13.1**	**12.5**
Standard Error of the mean	0.074	0.049	0.105	0.136

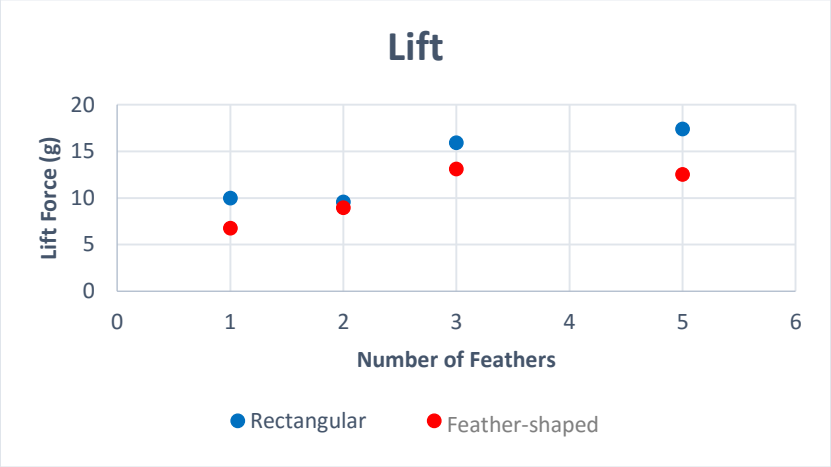

Table 3

Drag of Rectangular Extension configurations at 0º AOA

Trials	Drag with 1 Feathers (g) ± 0.1	Drag with 2 Feathers (g) ± 0.1	Drag with 3 Feathers (g) ± 0.1	Drag with 5 Feathers (g) ± 0.1
T1	2.1	2.6	3.6	4.4
T2	2.0	2.4	3.6	4.4
T3	1.9	2.6	3.5	4.3
T4	2.0	2.6	3.6	4.4
T5	2.0	2.5	3.5	4.3
T6	2.0	2.5	3.6	4.4
T7	1.9	2.5	3.4	4.3
T8	2.0	2.4	3.5	4.3
T9	2.0	2.5	3.6	4.3
T10	2.0	2.5	3.5	4.3
Average	**2.0**	**2.5**	**3.5**	**4.3**
Standard Error of the mean	0.017	0.022	0.021	0.016

Table 4

Drag of Feather-shaped Extension configurations at 0° AOA

Trials	Drag with 1 Feathers (g) ± 0.1	Drag with 2 Feathers (g) ± 0.1	Drag with 3 Feathers (g) ± 0.1	Drag with 5 Feathers (g) ± 0.1
T1	2.0	2.7	3.6	4.2
T2	1.9	2.7	3.5	4.2
T3	2.0	2.7	3.7	4.1
T4	1.8	2.7	3.6	4.0
T5	1.8	2.7	3.7	4.2
T6	1.8	2.7	3.6	4.2
T7	1.9	2.7	3.6	4.2
T8	1.9	2.7	3.7	4.1
T9	1.9	2.7	3.7	4.1
T10	1.9	2.6	3.6	4.1
Average	**1.9**	**2.7**	**3.6**	**4.1**
Standard Error of the mean	0.022	0.010	0.020	0.021

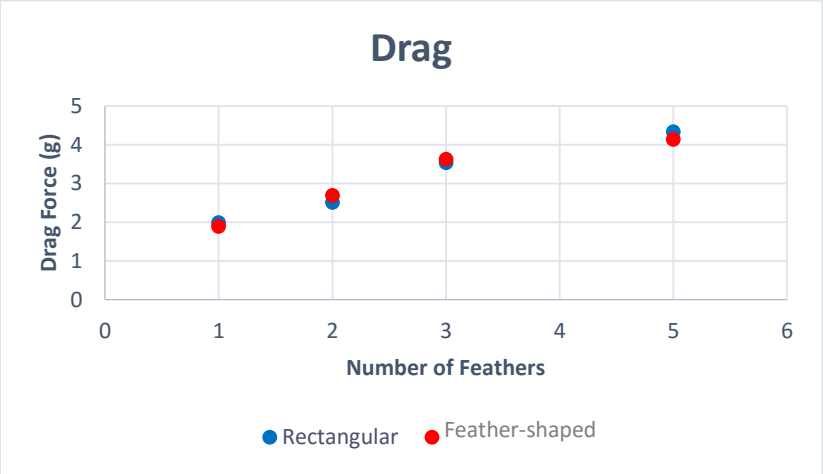

Table 5

L/D ratio of Rectangular Extension configurations at 0^o AOA

Trials	L/D with 1 Feathers	L/D with 2 Feathers	L/D with 3 Feathers	L/D with 5 Feathers
T1	4.86	3.92	4.44	4.00
T2	5.00	3.88	4.42	4.09
T3	5.05	3.65	4.49	3.95
T4	5.05	3.77	4.39	3.91
T5	4.90	3.76	4.60	4.00
T6	5.00	3.84	4.50	4.02
T7	5.21	3.68	4.62	4.02
T8	5.10	4.00	4.43	4.05
T9	5.00	3.84	4.42	4.05
T10	5.00	3.84	4.66	4.02
Average	**5.02**	**3.82**	**4.03**	**4.01**
Standard Error of the mean	0.029	0.034	0.029	0.015

Table 6

L/D ratio of Feather-shaped Extension configurations at 0^o AOA

Trials	L/D with 1 Feathers	L/D with 2 Feathers	L/D with 3 Feathers	L/D with 5 Feathers
T1	3.35	3.37	3.83	3.12
T2	3.63	3.37	3.69	3.14
T3	3.50	3.33	3.54	3.15
T4	3.50	3.30	3.56	3.15
T5	3.67	3.33	3.70	3.05
T6	3.61	3.41	3.61	2.86
T7	3.68	3.30	3.61	2.90
T8	3.63	3.33	3.49	2.95
T9	3.68	3.30	3.51	3.05
T10	3.47	3.31	3.58	2.93
Average	**3.57**	**3.34**	**3.61**	**3.03**
Standard Error of the mean	0.033	0.011	0.031	0.034

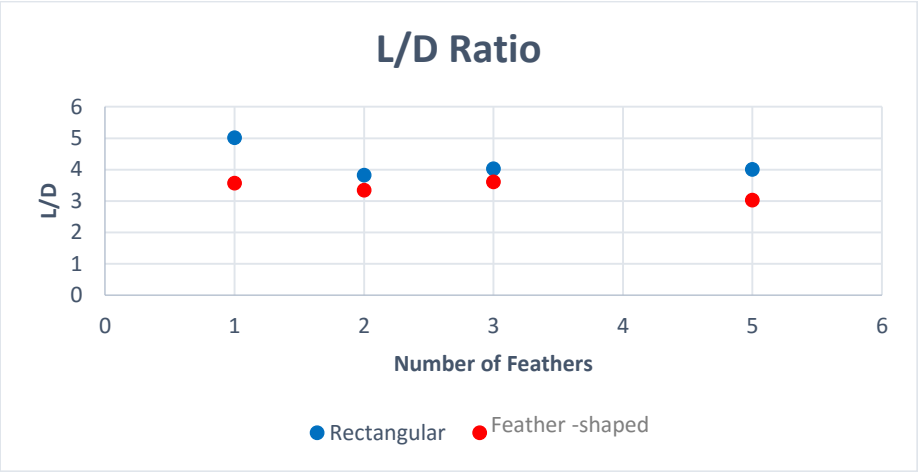
L/D Ratio
L/D
6
5
4
3
2
1
0
0
1
2
3
4
5
6
Number of Feathers
Rectangular
Feather -shaped

15 Degrees Angle of Attack

Table 7

Lift of Rectangular Extension configurations at 15^o AOA

Trials	Lift with 1 Feathers (g) ± 0.1	Lift with 2 Feathers (g) ± 0.1	Lift with 3 Feathers (g) ± 0.1	Lift with 5 Feathers (g) ± 0.1
T1	31.2	40.9	55.5	81.5
T2	31.8	43.3	53.7	82.9
T3	31.3	42.9	56.3	82.9
T4	31.7	42.5	56.8	83.8
T5	31.6	43.2	55.5	84.4
T6	31.2	42.8	56.2	83.8
T7	31.8	42.8	54.0	83.5
T8	31.2	41.9	54.5	82.6
T9	31.9	42.8	55.8	82.0
T10	31.3	42.2	54.9	82.6
Average	**31.5**	**42.53**	**55.32**	**83**
Standard Error of the mean	0.086	0.214	0.307	0.266

Table 8

Lift of Feather-shaped Extension configurations at 15^o AOA

Trials	Lift with 1 Feathers (g) ± 0.1	Lift with 2 Feathers (g) ± 0.1	Lift with 3 Feathers (g) ± 0.1	Lift with 5 Feathers (g) ± 0.1
T1	32.9	39.4	44.3	59.3
T2	33.7	39.8	45.8	59.5
T3	32.9	39.9	45	59.4
T4	33.2	40.1	44.9	60.6
T5	33.2	40	45	60.1
T6	33.1	40.2	45.5	60.3
T7	33.1	40	45.2	60.6
T8	33.2	39.9	45.2	60.9
T9	33.7	39.8	44.5	60.9
T10	32.9	39.7	45.4	59.9
Average	**33.19**	**39.88**	**45.08**	**60.15**
Standard Error of the mean	0.089	0.068	0.135	0.183

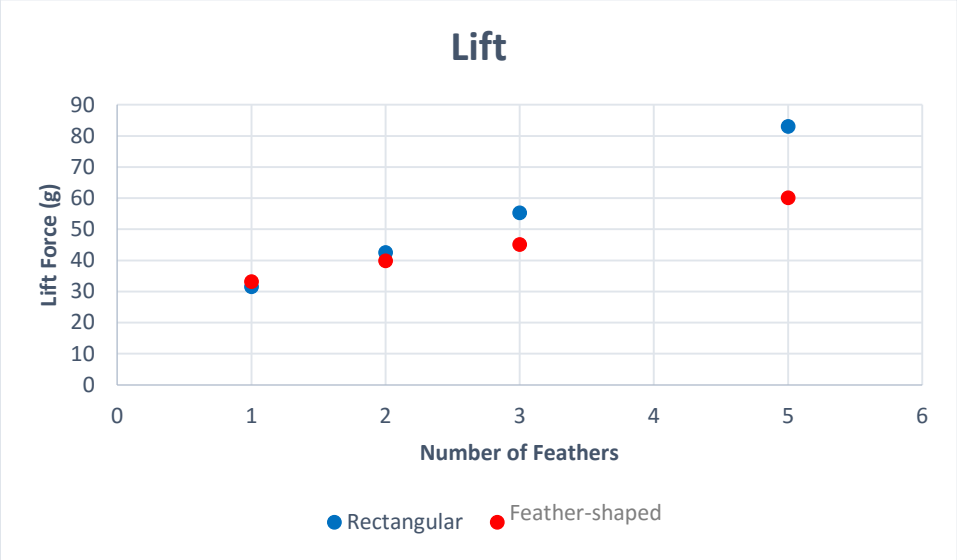

Table 9

Drag of Rectangular Extension configurations at 15º AOA

Trials	Drag with 1 Feathers (g) ± 0.1	Drag with 2 Feathers (g) ± 0.1	Drag with 3 Feathers (g) ± 0.1	Drag with 5 Feathers (g) ± 0.1
T1	13.5	17.5	21.8	34.2
T2	13.4	18.6	22.3	38.3
T3	13.3	18.3	22.2	38.7
T4	13.3	18.3	22.2	38.3
T5	13.3	18.2	21.5	37.9
T6	13.2	18.4	21.4	37.6
T7	13.5	18.6	21.5	36.4
T8	13.4	18	21.4	36.9
T9	13.5	18.5	21.9	35.7
T10	13.2	19	21.3	36.8
Average	**13.36**	**18.34**	**21.75**	**37.08**
Standard Error of the mean	0.035	0.120	0.114	0.417

Table 10

Drag of Feather-shaped Extension configurations at 15^{o} AOA

Trials	Drag with 1 Feathers (g) ± 0.1	Drag with 2 Feathers (g) ± 0.1	Drag with 3 Feathers (g) ± 0.1	Drag with 5 Feathers (g) ± 0.1
T1	12.5	15.6	18.7	26.2
T2	12.4	15.5	19.2	26.7
T3	12.5	15.5	19.2	26.3
T4	12.3	15.4	19.4	26.5
T5	12.4	15.1	19.1	26.5
T6	12.2	15.5	18.8	26.7
T7	12.5	15.6	19.1	26.5
T8	12.3	15.5	19.2	26.7
T9	12.3	15.6	19.6	26.8
T10	12.1	15.4	19.3	26.5
Average	**12.35**	**15.47**	**19.16**	**26.54**
Standard Error of the mean	0.041	0.045	0.079	0.057

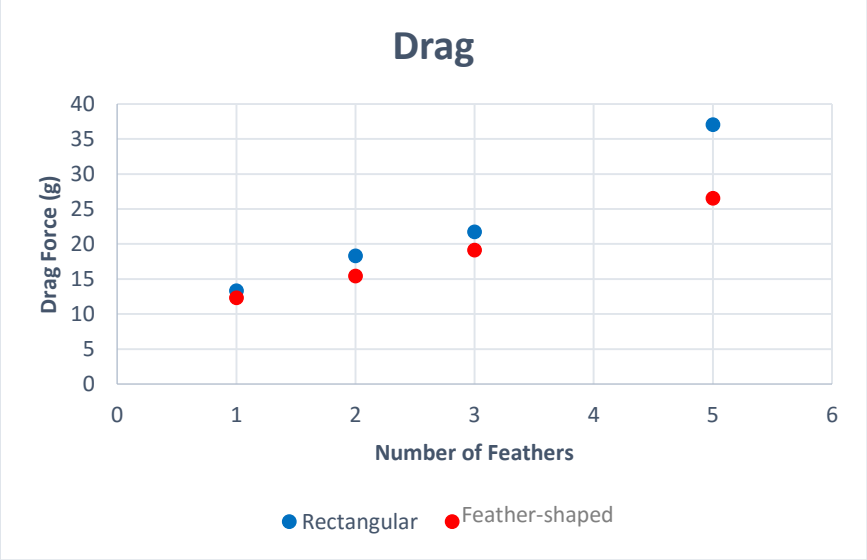

Table 11

L/D Ratio of Rectangular Extension configurations at 15^o AOA

Trials	L/D with 1 Feathers	L/D with 2 Feathers	L/D with 3 Feathers	L/D with 5 Feathers
T1	2.31	2.34	2.55	2.38
T2	2.37	2.33	2.41	2.16
T3	2.35	2.34	2.54	2.14
T4	2.38	2.32	2.56	2.19
T5	2.38	2.37	2.58	2.23
T6	2.36	2.33	2.63	2.23
T7	2.36	2.30	2.51	2.30
T8	2.33	2.33	2.55	2.24
T9	2.36	2.31	2.55	2.30
T10	2.37	2.22	2.58	2.24
Average	**2.357**	**2.319**	**2.546**	**2.241**
Standard Error of the mean	0.007	0.012	0.017	0.021

Table 12

L/D Ratio of Feather-shaped Extension configurations at 15^o AOA

Trials	L/D with 1 Feathers	L/D with 2 Feathers	L/D with 3 Feathers	L/D with 5 Feathers
T1	2.63	2.53	2.37	2.26
T2	2.72	2.57	2.39	2.23
T3	2.63	2.57	2.34	2.26
T4	2.70	2.60	2.31	2.29
T5	2.68	2.65	2.36	2.27
T6	2.71	2.59	2.42	2.26
T7	2.65	2.56	2.37	2.29
T8	2.70	2.57	2.35	2.28
T9	2.74	2.55	2.27	2.27
T10	2.72	2.58	2.35	2.26
Average	**2.69**	**2.58**	**2.35**	**2.27**
Standard Error of the mean	0.012	0.010	0.012	0.005

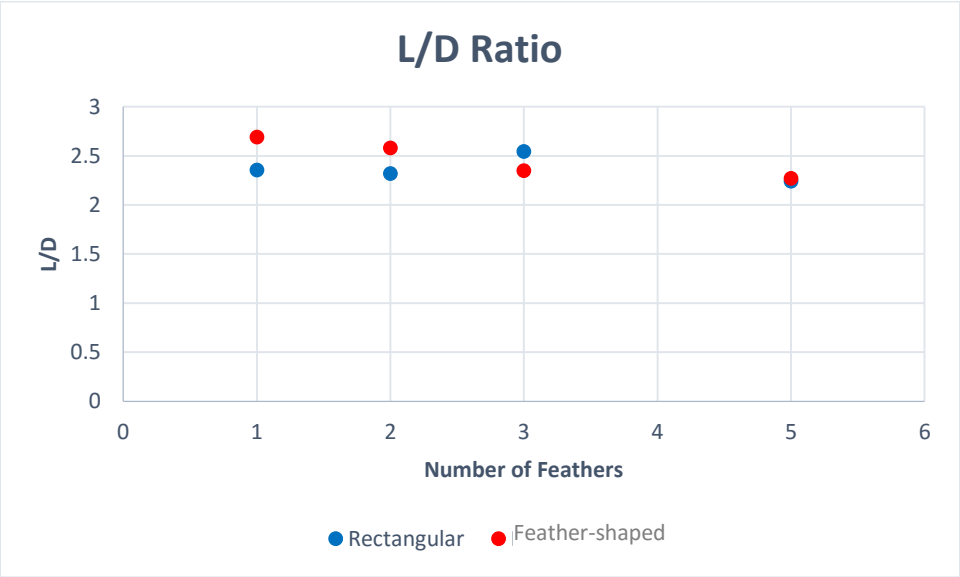
L/D Ratio
3
2.5
2
1.5
1
0.5
0
L/D
0
1
2
3
4
5
6
Number of Feathers
Rectangular
Feather-shaped

References

1. Tucker, Vance A. "Gliding Birds: Reduction of Induced Drag by Wing Tip Slots between the Primary Feathers." *Journal of Experimental Biology* (1993): 1-26. pdf file.
2. "Aerodynamics of Wing Vortices." *General Aviation Portal Fixed Wing Flight Training*. N.p., 2000. Web. 13 Jan. 2016. <http://www.pilotfriend.com/training/flight_training/aero/wng_vort.htm>.
3. Alexander, David E., and Steven Vogel. *Nature's Flyers*. N.p.: Johns Hopkins UP, n.d. Print.
4. Chun-Mei, Xie, and Huang Wei-Xi. "Vortex interactions between forewing and hindwing of dragonfly in hovering flight." *Theoretical and Applied Mechanics Letters* 5.1 (2015): 24-29. *Science Direct*. Web. 22 Jan. 2016. <http://www.sciencedirect.com/science/article/pii/S2095034915000136>.
5. Larson, George C. "How Things Work: Winglets." *Air and Space Smithsonian* Sept. 2001: n. pag. Web. 18 Mar. 2015. <http://www.airspacemag.com/flight-today/how-things-work-winglets-2468375/?no-ist>.
6. Zakarowsky, Sheri. "The Lift Equation." *The Glenn Research Center: Beginner's Guide to Aerodynamics*. Ed. Tom Benson. National Aeronautics and Space Administration, 12 June 2015. Web. 22 Jan. 2016. <https://www.grc.nasa.gov/www/K-12/airplane/lifteq.html>.

7. Hall, Nancy, ed. "The Drag Equation." *The Glenn Research Center: Beginner's Guide to Aerodynamics.* Ed. Tom Benson. National Aeronautics and Space Administration, 5 May 2015. Web. 17 Jan. 2016. <https://www.grc.nasa.gov/www/k-12/airplane/drageq.html>.
8. Hall, Nancy, ed. "Induced Drag Coefficient." *The Glenn Research Center: Beginner's Guide to Aerodynamics*. Ed. Tom Benson. National Aeronautics and Space Administration, 5 May 2015. Web. 23 Jan. 2016. <https://www.grc.nasa.gov/www/k-12/airplane/induced.html>.
9. Hall, Nancy, ed. "Vector balance of Forces for a Glider." *The Glenn Research Center: Beginner's Guide to Aerodynamics*. Ed. Tom Benson. National Aeronautics and Space Administration, 5 May 2015. Web. 11 Jan. 2016. <https://www.grc.nasa.gov/www/k-12/airplane/glidvec.html>.
10. U.S Fish ad Wildlife Service. "*California Condor Primary Wing Feathers.*" Infographic. The Feather Atlas. U.S Fish and Wildlife Service, 2 May 2013. Web. 18 Mar. 2015. <http://www.fws.gov/lab/featheratlas/feather.php?Bird=CALC_primary_adult>.
11. Ehrlich, Paul R., David S. Dobkin, and Darryle Wheye. "Wing Shapes and Flight." *Birds of Stanford*. San Jose: Stanford University, 1999. *Birds of Stanford*. Web. 18 Mar. 2015. <https://web.stanford.edu/group/stanfordbirds/text/essays/Wing_Shapes.html>.
12. Homer, David, and Michael Bowen-Jones. *Physics Course Companion*. 2014 ed. Oxford: Oxford UP, 2014. Print.
13. Vogel, Steven. *Life in Moving Fluids*. 2nd ed. N.p.: Princeton UP, 1996. Print.